Missing rows on oxygen-covered Cu(100) vicinal surfaces: a scanning tunnelling microscopy investigation

1997 J. Phys.: Condens. Matter 9 21

(http://iopscience.iop.org/0953-8984/9/1/005)

J. Phys.: Condens. Matter **9** (1997) 21–31. Printed in the UK PII: S0953-8984(97)77136-4

Missing rows on oxygen-covered Cu(100) vicinal surfaces: a scanning tunnelling microscopy investigation

P J Knight, S M Driver and D P Woodruff
Physics Department, University of Warwick, Coventry CV4 7AL, UK

Received 13 August 1996, in final form 25 October 1996

Abstract. Scanning tunnelling microscopy images of oxygen-covered Cu(410) facets, of the Cu(100)($\sqrt{2}\times 2\sqrt{2}$)R45°–O structure, and of the faceting of Cu(610) in the presence of adsorbed oxygen have been used to investigate the basic elements of the atomic-scale structure of these surfaces. The existence of stable (100) nanofacets of widths corresponding to those of ($4n$ 1 0) ($n = 2, 3, \ldots$) faces is shown to be consistent with a common structural model for all of these surfaces based on the well known structural unit of three adjacent [001] Cu atom rows and one missing row which comprises the Cu(100)($\sqrt{2}\times 2\sqrt{2}$)R45°–O surface. This model implies that on the (410) surface the missing row lies at the bottom of each atomic step on this surface. All these structures have a common local geometry for the adsorbed O atoms coordinated to four Cu atoms.

1. Introduction

It is now well established that oxygen chemisorption on both Cu(100) and (110) surfaces leads to substantial reconstruction of the outermost Cu atom layer which has a lower atomic density than that of the clean surface. In the case of Cu(110) the equilibrium (2×1)–O phase can be thought of as a 'missing row' structure with every other [001] Cu atom row absent, while the O atoms occupy near-collinear long-bridge sites in the remaining rows [1–8], although the actual mechanism of formation of this structure has been found to be by adding, rather than removing, Cu atom rows [7, 8]. On Cu(100), oxygen induces a ($\sqrt{2} \times 2\sqrt{2}$)R45°–O reconstruction involving the removal of every fourth Cu [001] atom row; the O atoms in this structure occupy the sites along the edges of the missing row near coplanar with the remaining top-layer Cu atoms as shown in figure 1(a) [9–15]. In both cases approximately linear Cu–O–Cu–O chains are present on the surface, although the actual local Cu coordination number of the O atoms is not two but four—on (110) this comprises two Cu neighbours in the top Cu layer and two in the second layer, while on (100) there are three Cu neighbours in the top layer and one in the second layer. The local bond angles of the O sites on the two reconstructed surfaces are also almost identical [16].

In addition to this well established oxygen-induced reconstruction of these two low-index faces of Cu, oxygen adsorption on Cu(100) vicinals is also known to cause faceting to Cu(410) [17–21]. Indeed, one factor which led to the original idea [15] of a possible missing row structure for the (100)($\sqrt{2} \times 2\sqrt{2}$)R45°–O phase was the analogy with the highly stable oxygen-covered Cu(410) surface. On this surface there is limited evidence that at least some of the chemisorbed O atoms occupy step edges sites [22], while the

0953-8984/97/010021+11$19.50

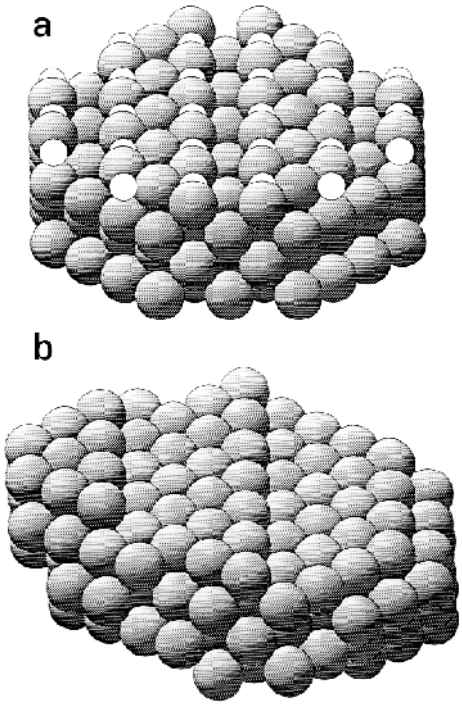

Figure 1. Atomic hard-sphere models of (a) Cu(100)($\sqrt{2} \times 2\sqrt{2}$)R45°–O (O atoms represented by the smaller lighter spheres) and (b) the clean Cu(410) surface. In both cases the models do not show any possible lateral relaxation of the atomic positions at the step or missing row edges.

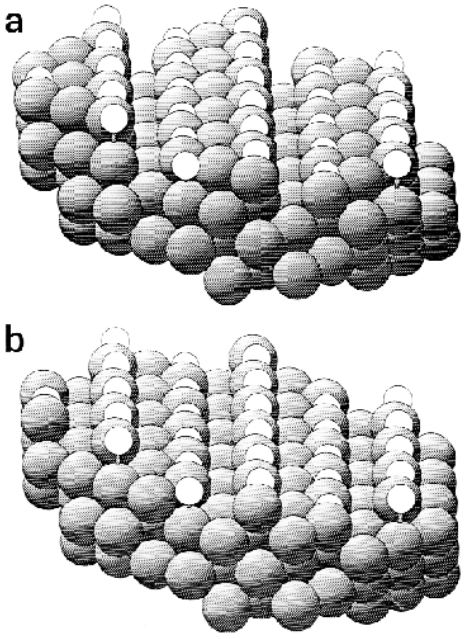

Figure 2. Atomic hard-sphere models of different missing row Cu(410) structures: (a) down-step missing row [11] and (b) mid-terrace missing row [23]. No lateral relaxation of the atomic positions at the edges of the steps or missing rows is included.

terrace width is identical to the periodicity of the (100)($\sqrt{2} \times 2\sqrt{2}$)R45°–O phase (see figure 1(a) and (b)), so a missing row on (100) opens up similar 'step-edge' sites. More recently, however, this argument has been inverted by suggesting that the stable oxygen-covered Cu(410) surface may itself have one missing row per (100) terrace. Two possible locations of this missing row have been considered. One of these, with the missing row at the bottom of the step—i.e. the row on the terrace furthest from the step down off this terrace (figure 2(a)), was proposed by Robinson *et al* [11] in discussing x-ray diffraction data from the (100)($\sqrt{2} \times 2\sqrt{2}$)R45°–O phase. The other model, in which the second row of the terrace behind the step edge is removed (figure 2(b)), was proposed on the basis of an early scanning tunnelling microscopy (STM) study from our own group [23]. For convenience we will refer to these two models in the remainder of this paper as having a down-step missing row or a mid-terrace missing row respectively.

As part of a much more detailed STM study of oxygen-induced Cu(610) faceting we have collected further information on this issue, not only through higher-resolution images of the oxygen-covered Cu(410) facets themselves, but also by investigating both the stability and high-resolution images of other nearby vicinal surfaces. Despite the considerable potential ambiguity of the interpretation of atomic-scale STM images in terms of atomic positions, we believe that these new data provide strong support for the original down-step missing row model of the Cu(410)/O surface proposed by Robinson *et al*.

2. Experimental details

The experiments were conducted in an ultra-high-vacuum (UHV) STM instrument manufactured by Omicron. The STM itself comprises a single piezo-electric tube scanner with stick–slip piezo-electric coarse tip approach and coarse lateral movement (the Omicron 'Micro-STM') mounted on a magnetically damped spring suspension. The instrument also incorporates low-energy electron diffraction (LEED) optics with which to assess the state of the surface. Ion bombardment and sample heating is also provided with the sample in the precharacterization chamber prior to transfer onto the STM stage. STM tips were prepared from 0.25 mm diameter polycrystalline tungsten wire. This wire was first annealed to approximately 1200 °C for 1 min at a pressure of 2×10^{-5} mbar. The tips were then prepared either by etching in 0.6 M KOH (15 V a.c.) or cutting at an oblique angle with wire cutters. Once mounted on the piezo-scanner, tips were conditioned in the UHV microscope by a combination of frequent 10 V pulses (1 s) and more occasional high-voltage field evaporation (300 V at 20 nA for approximately 15 min).

The nominal (610) orientation copper crystal was spark-machined from a single-crystal bar after x-ray Laue orientation, and subsequently mechanically polished with successively finer grades of diamond paste prior to mounting in the UHV system. Subsequent argon ion bombardment (650 eV) and annealing (to 650–700 °C) cycles led to a clean surface showing a LEED pattern with the characteristic split diffraction beams (see e.g. [19]) to be expected from a (610) orientation. This method of preparation was found to yield a clean surface as judged by Auger electron spectroscopy performed using the LEED optics as a retarding field analyser. STM observations were made after different oxygen exposures and annealing sequences (typically checked by LEED) as described in the following sections. Oxygen exposures were achieved by simply introducing research-grade purity O_2 gas into the sample chamber to a pressure of around 10^{-6} mbar, monitored using an *in situ* quadrupole mass spectrometer. The LEED and STM studies revealed that the actual average orientation of the surface differed slightly from that of (610) in that the tilt away from (100) was some 10° out of the [001] zone. As a consequence, the oxygen-covered surfaces showed step edges not only along [001] but also along [010]. This slight miscut is not relevant to the subject of this paper.

3. Results and discussion

We first consider the atomic-scale images of fully faceted Cu(410)–O regions obtained after elevated-temperature oxygen exposures and rehearse some of the arguments concerning the atomic-scale structure of the surface which might be obtained from such images. For this purpose we refer particularly to the high-resolution STM images shown in figure 3 of the Cu(410)–O and Cu(100)($\sqrt{2} \times 2\sqrt{2}$)R45°–O surfaces, together with the model structures of figures 1(a) and 2. Two important issues need to be recognized in this discussion. The first is that in recording STM images of such surfaces there is no unique appearance to the images. In the present case the differences obtained are almost certainly more to do with the tip condition than the tunnelling conditions. Generally, for any particular tip condition, the images obtained from these surfaces were insensitive to both the polarity and magnitude of the bias voltage in the range of these conditions giving atomic-scale resolution. The most 'typical' images of the oxygenated (410) surface comprise rows of bright spots which exactly define the primitive unit mesh of the surface, but closer inspection typically reveals more detail within this unit mesh, providing information on the structure of the (100) terraces. This variation is generally attributed to the shape of the tip. Even with a relatively imperfect

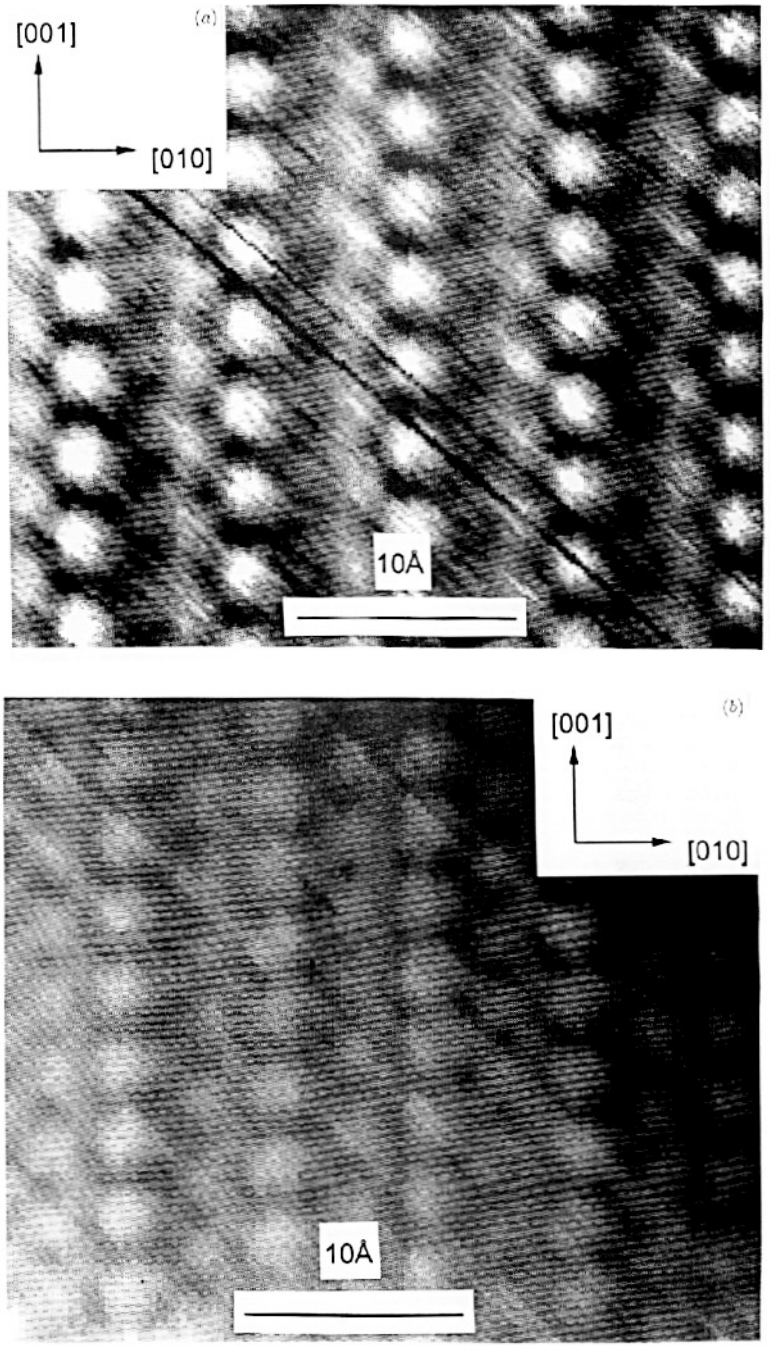

Figure 3. Small-area STM images of Cu(410)–O under different tip conditions. (a) and (b) show images with some additional mid-terrace features, (b) being most typical, while (c) shows an example of the images showing the largest amount of mid-terrace detail. Also shown (d) is a typical 'dimer' image of the $(\sqrt{2} \times 2\sqrt{2})R45^{\circ}$–O structure on Cu(100). Tunnelling conditions of sample bias and current were the following: (a) −2 mV, 13 nA; (b) −0.60 V, 1.5 nA; (c) −1 mV, 7.4 nA; (d) −0.14 V, 1.0 nA.

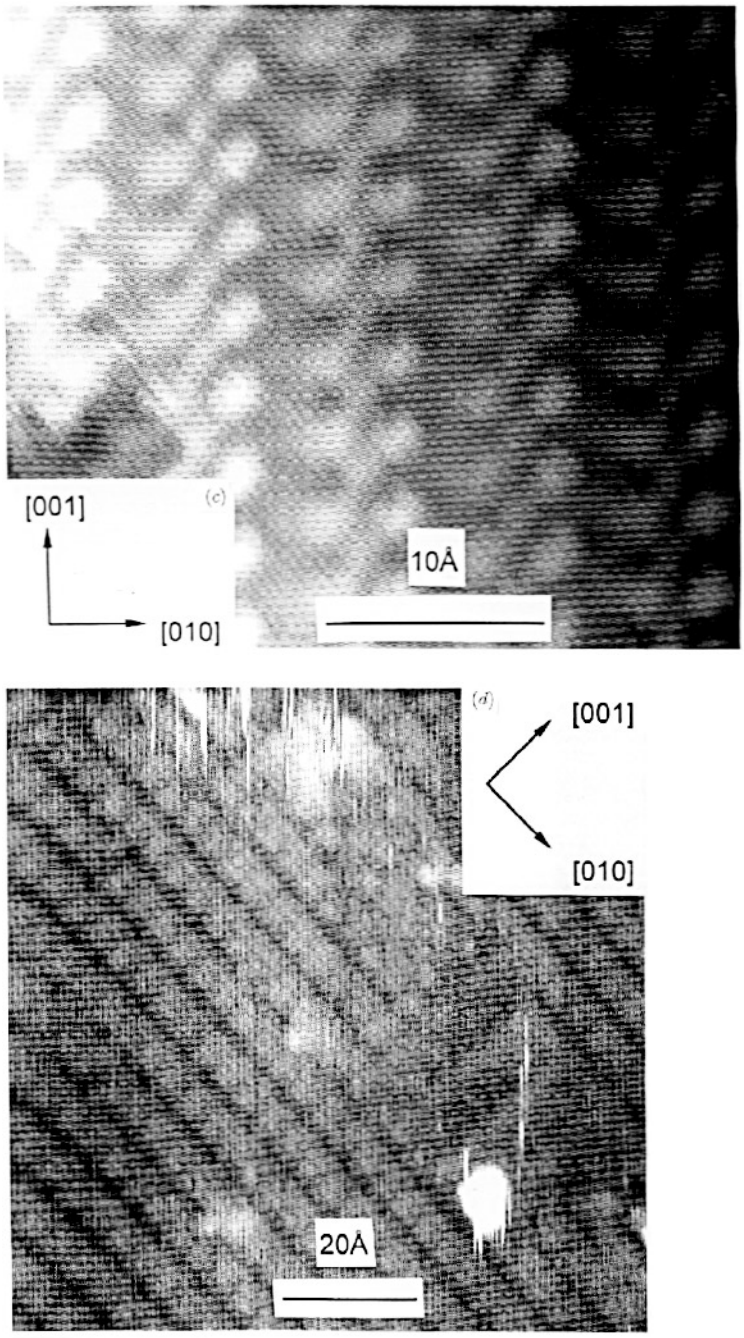

Figure 3. (Continued)

tip one can expect to image the large step-edge corrugations defining the long side of the unit mesh. By contrast, a suitably located asperity is needed on the tip to image detail on the terrace, especially as one approaches the down-step corner. For this reason, one

might assume that the images showing the greatest detail are the most representative of the highest-resolution 'true' images. We will work, with some caveats, on this basis. We show, however, not only images at this highest resolution (figure 3(c)), but also two further images (figure 3(a) and (b)) which resolve selectively different components of this 'optimum' image. The second problem, of course, is the actual atomic-scale interpretation of the images. Are the highest points (the bright regions) above the locations of Cu atoms, or of O atoms, or of some points of charge pile-up in-between? In this regard there is some evidence, at least for the oxygen-covered Cu(110) surface, that the most common high-resolution images (probably obtained using oxygen-terminated tips [24]) are consistent with asperities correlating with Cu atoms, the O atoms being 'invisible' under these circumstances. With even more caution we will use this as the basis of an initial evaluation.

In order to try to avoid this problem of assigning the image asperities to specific atoms, the original STM study [23] concentrated on the apparent spacing of the double rows seen in the images of each terrace. It was argued, in particular, that any missing row would cause lateral relaxation of atoms into the space left by the missing row, leading to an apparent change in the row spacing. On this basis the fact that the two closest rows were on the top of the step was taken to imply that the missing row lay just behind the step edge (in the mid-terrace site of figure 2(b)). Figure 3(b) shows an image taken from our more recent work which is consistent with this argument. By contrast, however, the image showing the greatest detail on the (100) terraces (figure 3(c)) shows three rows of asperities with the middle row offset by a half the periodicity along the step-edge direction. If we assume that the asperities in this image do correspond to atomic positions of one elemental species, we can only interpret it in terms of Cu atom sites with *no* missing row in this location. A missing row is possible in the down-step location (figure 2(a)); certainly no row of asperities is seen here, although this row, if it were present, would be the most demanding to image because of its down-step location.

One important feature of the down-step missing row model for the oxygenated (410) surface which is apparent from a comparison of figures 1(a) and 2(a) is that the basic 'building block' which forms the outermost layer of this surface is identical to that of the Cu(100)($\sqrt{2} \times 2\sqrt{2}$)R45°–O structure, namely three adjacent [001] Cu atom rows with oxygen atoms decorating the outer step edges. We might therefore ask how the STM images of these two structures compare. Of course, a key difference is that on the (100) surface these building blocks are coplanar, whereas on the (410) surface they are displaced perpendicular as well as parallel to the (100) terraces. In fact, the most common appearance of the published STM images of the (100)($\sqrt{2} \times 2\sqrt{2}$)R45°–O phase [10, 12] is of bright 'dimer' rows along a ⟨100⟩ direction, similar to the image shown in figure 3(d). It is not actually clear whether the 'dimer pairing' seen in these images is across the missing row or across the three-row building block, nor, indeed, whether the image asperities correspond to O atoms or the Cu edge atoms along the sides of the missing rows. Without any lateral relaxation of either the atomic positions or the electron charge distribution imaged in the STM, the Cu–Cu or O–O distances across the missing rows and across the three-row building blocks should be identical. Including relaxation which might be expected to cause movement of (Cu and O) atoms and associated valence charge into the space vacated by the missing Cu atom row leads to the conclusion that the 'dimers' of the image straddle the missing row, and this is the interpretation which has been applied in the earlier work. This kind of relaxation argument was used in the original interpretation of the earlier STM images from Cu(410)–O in terms of a mid-terrace missing row, although the Cu(410)–O images never show the pronounced streaking into unresolved dimers which characterizes most of the images from the (100) surface. This latter observation may imply that there is

not a missing row in a mid-terrace position on the (410)–O surface. Note in this regard that if the (410)–O surface has a down-step missing row dimer, images of the kind seen on the (100) surface would not be expected on the (410)–O surface, as the local geometry on one side of the missing row is quite different.

Although the dimerized appearance is most characteristic of the published STM images of the Cu(100)($\sqrt{2} \times 2\sqrt{2}$)R45°–O surface, there are examples of images showing further detail ('higher-resolution' images) which show a remarkable similarity to the highest-resolution image (figure 3(c)) which we obtain from the Cu(410)–O surface. We have not made an extensive study of the Cu(100) surface and the best example of this kind of image is in a recent paper by Leibsle [25]. Leibsle's images not only show dimer regions but also regions in which it is possible to resolve an extra row of asperities between the dimers, producing an image perfectly consistent with the known structure of the ($\sqrt{2} \times 2\sqrt{2}$)R45°–O structure if one assumes the STM asperities are Cu atom positions as suggested earlier. These images are also consistent with the interpretation of the lower-resolution dimer images as having the missing row positioned such as to bisect all the dimers as has previously been supposed.

If we accept that the most detailed STM images are representative of the highest-resolution data, the images of figure 3(c) and of Leibsle from Cu(100) provide a clear basis for resolving the structure of the Cu(410)–O surface in favour of the down-step missing row model of figure 2(a). Specifically, both images show asperities which can be associated with the Cu atoms of the basic three-row building block of both of these structures. At this point we should also remark that another STM study of Cu(410)–O, which has recently come to our notice and was conducted concurrently with our own work, has also been interpreted as favouring this model on the basis of images somewhat similar to, but lacking the full detail of, figure 3(c) [26].

While these data and the associated discussion clearly favour the down-step missing row model, this interpretation does introduce explicitly an assumption as to which parts of the surface (specifically the Cu atoms) correlate with the STM asperities. Our experiments, however, have provided further strong indirect support for the down-step missing row model without any need to interpret the details of the STM images so explicitly. Figure 4(a) shows a larger-area STM image of another part of the Cu(610) surface following the elevated-temperature oxygen exposure which provides the basis of this further information. In this image one sees how part of the surface achieves the average (610) orientation despite the formation of large (410) facets. Although regions are seen in which several [001] steps occur at spacings corresponding to that of a (410) face, there are also larger spacings corresponding to wider strips of (100) terrace or (100) 'nano-facets'. What is notable about these wider terraces, however, is that their width is always an integral multiple of the width of the (410) terrace of four [001] Cu atom rows. A wider search of many images reveals that this behaviour is characteristic, with only occasional terrace widths comprising an even number of Cu atom rows which is not an integral multiple of four, and no examples of an odd number of Cu atom rows. This basic phenomenon also holds for the Cu(610) surface after exposure to a saturation coverage of oxygen at room temperature. In this case (410) faceting also occurs, but the average facet size is much smaller—typically only a few (less than 10) step spacings in width, compared with hundreds to thousands of step spacings in width after annealing briefly above 250 °C. In between these small (410) facets are even narrower regions of extended (100) terrace to retain the original average orientation, but these (100) regions also have widths of an integral multiple of the four-row unit which comprises the (410) surface. An image of such a region following room-temperature oxygen exposure is shown in figure 4(b), while part of this image is

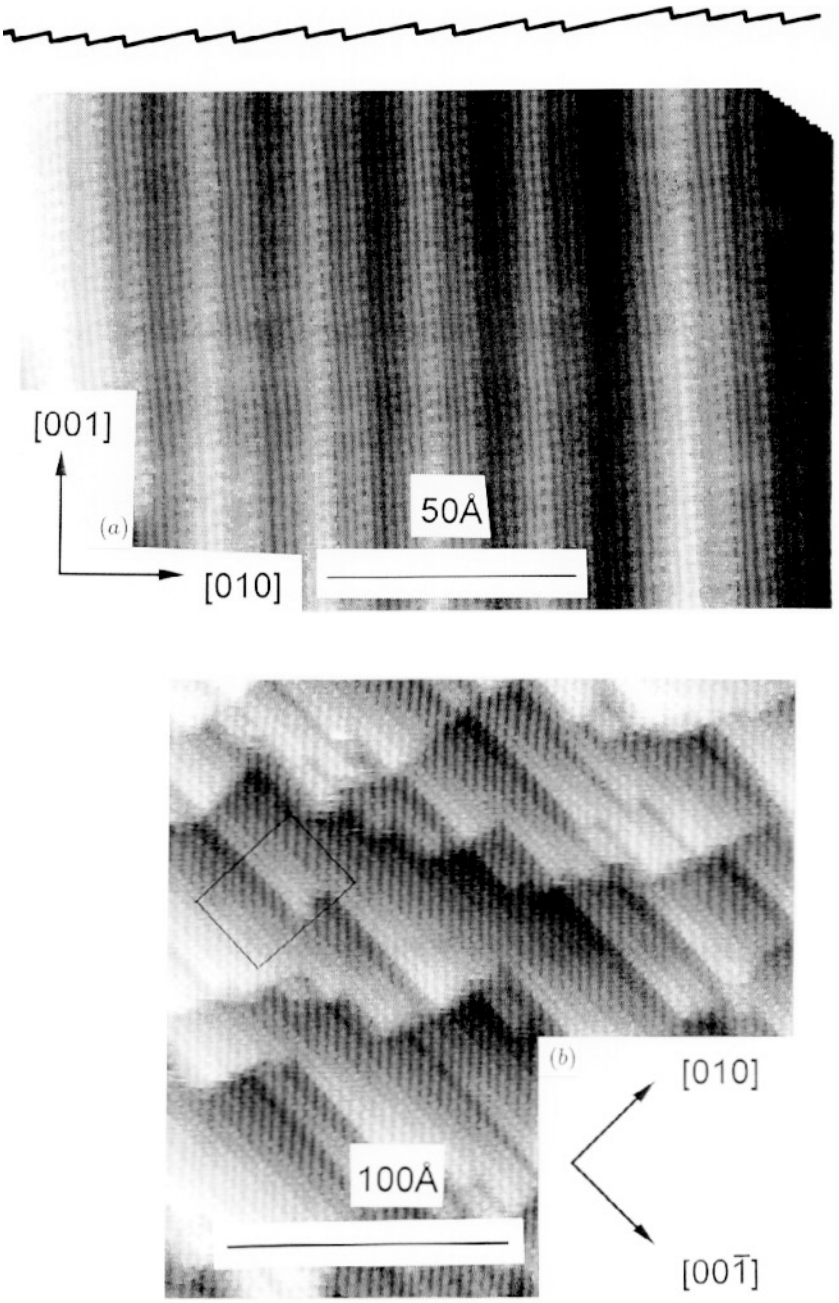

Figure 4. STM images of the faceted Cu(610)–O surface, showing (410) regions (short step spacing) and wider (100) terraces of (4*n* 1 0) character. (a) Shows a nanofaceted region of an annealed surface. The schematic section above this image shows the extended (810) and (12 1 0) character (100) nanofacets. (b) An unannealed surface; (c) at higher magnification the boxed area of (b) comprising a (810) nanofacet surrounded by more extended facets of regular steps corresponding to (410). Tunnelling conditions of sample bias and current were the following: (a) −0.10 V, 1.8 nA; (b) and (c) −0.67 V, 1.5 nA.

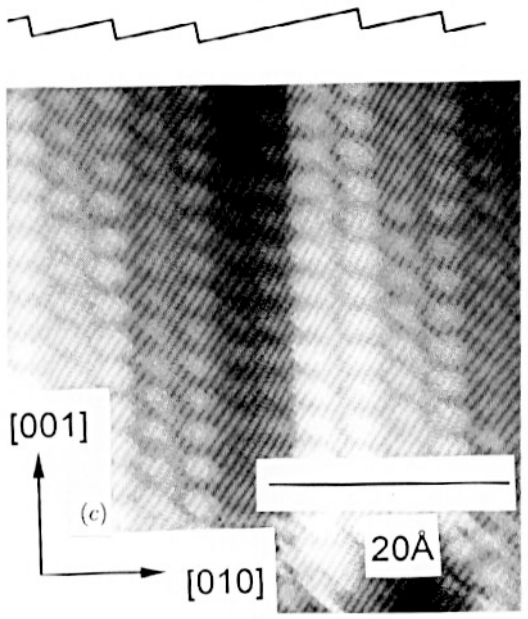

Figure 4. (Continued)

shown at higher magnification in figure 4(c). In figure 4(c) two narrow regions of (410) are separated by a strip of (100) terrace eight Cu atom rows wide—equivalent to a single terrace of a Cu(810) surface. The STM image clearly resolves atomic-scale detail in this widened terrace.

In considering the interpretation of this image we should note that one can reasonably expect the presence of at least one missing row to reflect the (100) character and the tendency to form a local $(\sqrt{2} \times 2\sqrt{2})$R45°–O structure. In addition, of course, one might expect the regions of this terrace closest to the step edges to reconstruct in a fashion similar to that of the terraces on the (410) surface. Figure 5 shows the basic structure of such a region of an ideal clean surface (a) and two possible models of this region of surface after oxygen adsorption, one (b) based on a down-step missing row for the (410) surface, the other (c) based on a mid-terrace missing row. The lighter shaded atoms in these models could be correlated with the asperities seen in the image of figure 4(c). The attraction of the down-step missing row model is immediately obvious from figure 5. The whole surface is still made up from the three-row building block of the $(\sqrt{2} \times 2\sqrt{2})$R45°–O surface. Moreover, adding extra units of this building block (plus the associated missing row) to the width of the (100) terrace increases the width in units of four Cu atom rows, providing a rationale for the stability of the (4*n* 1 0) structures.

One final comment is appropriate concerning the nature of the stable Cu–O structural element on all known Cu surface oxygen chemisorption-induced reconstructions. In the earlier STM study, and in many other papers (see e.g. [26, 27]), the stability of the Cu–O–Cu–O structural unit has been stressed. Cu–O–Cu–O chains have even been found to grow on Ag(110) [28]. Such a unit occurs at the step edge in the mid-terrace missing row model of figure 2(b). An alternative view [16], however, is that the key structural element involves O sites which are fourfold Cu-coordinated and these are present on both

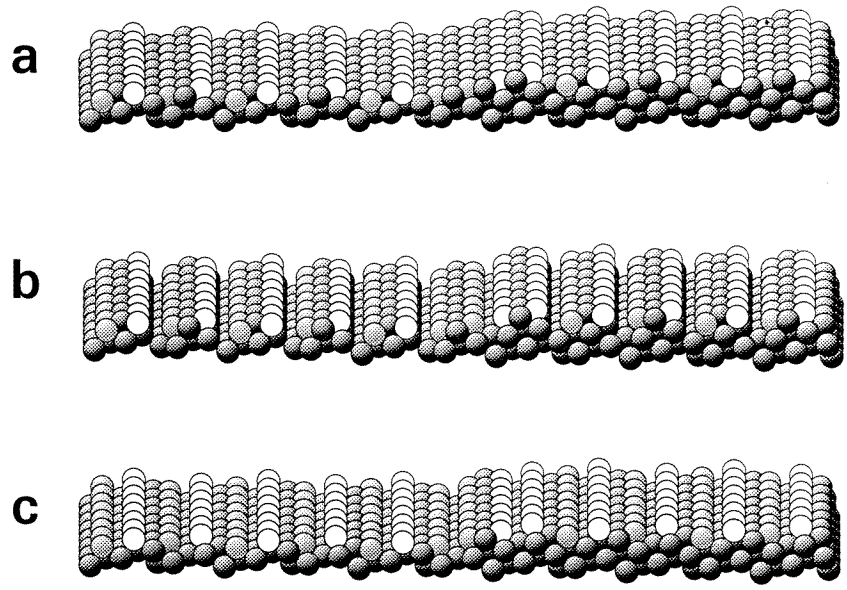

Figure 5. Hard-sphere models of an area of a Cu(n10) surface comprising a (100) terrace having twice the width of those in (410) (i.e. the terrace width of (810)) abutting regions of (410) surface as seen in figure 4(b): (a) an ideal unreconstructed surface, (b) based on a model consistent with down-step missing rows on the (410) surface; (c) based on a mid-terrace missing row model for this same surface. For clarity only Cu atoms are shown, and those atom rows which appear to be imaged in the STM are shown lighter. Note that in the reconstruction models all of these lighter Cu atom rows would be expected to comprise Cu–O–Cu–O chains, so the STM images of figures 4 and 3(b) could equally well be interpreted in terms of O atom sites in these rows. Figure 3(a) and (c), however, appear to be *only* interpretable in terms of Cu atom positions as discussed in the text.

Cu(110)(2×1)–O and $(\sqrt{2} \times 2\sqrt{2})$R45°–O. The conclusions of the present paper appear to favour this alternative view. We should note, in particular, that a single [001] Cu–O–Cu–O atom chain on any fcc (110) surface (including Cu(110) and Ag(110)) provides fourfold coordinated sites for the O atoms. However, this is not true for a [001] Cu–O–Cu–O atom chain on a (100) surface, in which the O atoms lie atop single Cu atoms in the underlying top substrate layer; the O atoms are therefore only threefold coordinated to the metal atoms and an adjacent Cu atom chain is required to make up the missing fourth neighbour.

4. Conclusions

A comparison of the highest-resolution STM images of oxygen-covered Cu(410) surfaces and of Cu(100)$(\sqrt{2} \times 2\sqrt{2})$R45°–O indicates that the most probable structural model for the (410) surface is one in which a [001] Cu atom row is missing from immediately below each step edge, and that the images correspond to asperities over each Cu atom in the surface layer. Oxygen-induced faceting of a Cu(610) surface reveals that, in addition to the dominant (410) facets, (100) nanofacets occur which are found to have widths which are integral multiples of the width of the terraces on the (410) surface which are themselves composed of four Cu [001] rows. The intrinsic stability of these local (4n 1 0) regions in the presence of chemisorbed oxygen provides further indirect support for the down-step

missing row model of the (410) face, and offers a unified description of the stable structural element in oxygen-covered Cu(100) and (4*n* 1 0) faces in terms of three [001] Cu atom rows separated by a missing row and having oxygen atoms adsorbed along the edges of these Cu strips in fourfold coordinated sites.

Acknowledgments

The authors are pleased to acknowledge the SERC, and latterly the EPSRC (Engineering and Physical Science Research Council) for a research grant for instrumentation and the support of PJK as a research assistant, and for a research studentship for SMD. They also acknowledge Peter Varga, Michael Schmidt and their colleagues at the TU Wien for their valuable contribution to the effective commissioning of our STM instrument.

References

[1] Bader M, Puschmann A, Ocal C and Haase J 1986 *Phys. Rev. Lett.* **57** 3273
[2] Yarmoff J A, Cyr D M, Huang J H, Kim S and Williams R S 1986 *Phys. Rev.* B **33** 3856
[3] Robinson A W, Somers J S, Ricken D E, Bradshaw A M, Kilcoyne A L D and Woodruff D P 1990 *Surf. Sci.* **227** 237
[4] Feidenhans'l R, Grey F, Johnson R L, Mochrie S G J, Bohr J and Nielsen M 1990 *Phys. Rev.* B **41** 5420
[5] Parkin S R, Zeng H C, Zhou M C and Mitchell K A R 1990 *Phys. Rev.* B **41** 5432
[6] Durr H, Fauster Th and Schneider R 1991 *Surf. Sci.* **244** 237
[7] Coulman D J, Wintterlin J, Behm R J and Ertl G 1990 *Phys. Rev. Lett.* **64** 1761
[8] Jensen F, Besenbacher F, Lagsgaard E and Stensgaard I 1990 *Phys. Rev.* B **41** 10 233
[9] Zeng H C, McFarlane R A and Mitchell K A R 1989 *Surf. Sci.* **208** L7
[10] Woll Ch, Wilson R J, Chiang S, Zeng H C and Mitchell K A R 1990 *Phys. Rev.* B **42** 11 926
[11] Robinson I K, Vlieg E and Ferrer S 1990 *Phys. Rev.* B **42** 6954
[12] Jensen F, Besenbacher F, Lagsgaard E and Stensgaard I 1990 *Phys. Rev.* B **42** 9206
[13] Zeng H C and Mitchell K A R 1990 *Surf. Sci.* **239** L571
[14] Atrei A, Bardi U, Rovida R, Zanazzi E and Casalone G 1990 *Vacuum* **41** 333
[15] Asensio M C, Ashwin M J, Kilcoyne A L D, Woodruff D P, Robinson A W, Lindner Th, Somers J S, Ricken D E and Bradshaw A M 1991 *Surf. Sci.* **236** 1
[16] Liu W, Wong K C, Zeng H C and Mitchell K A R 1995 *Prog. Surf. Sci.* **50** 247
[17] Berndt W 1967 *Z. Naturf.* a **22** 1655
[18] Trepte L, Menzel-Kopp C and Menzel E 1967 *Surf. Sci.* **8** 223
[19] Perdereau J and Rhead G E 1971 *Surf. Sci.* **24** 555
[20] Boulliard J C, Domange J L and Sotto M 1986 *Surf. Sci.* **165** 434
[21] Sotto M 1992 *Surf. Sci.* **260** 235
[22] Thompson K A and Fadley C S 1984 *Surf. Sci.* **146** 261
[23] Lloyd G W and Woodruff D P 1993 *Surf. Sci.* **285** L503
[24] Ruan L, Besenbacher F, Stensgaard I and Lagsgaard E 1993 *Phys. Rev. Lett.* **70** 4079
[25] Leibsle F 1996 *Surf. Sci.* **337** 51
[26] Reiter S and Taglauer E 1996 *Surf. Sci.* at press
[27] Woodruff D P 1994 *J. Phys.: Condens. Matter* **6** 6067
[28] Matsumota Y and Tanaka K 1996 *Surf. Sci.* **350** L227 and references therein